

Observation of B_s mesons in $p\bar{p}$ collisions at $\sqrt{s} = 1.8$ TeV

A. Vitarana (pemb5671)

Abstract

The observation of the strange B mesons (B_s) is presented with a data sample corresponding to an integrated luminosity of 28 pb^{-1} for 1.8 TeV $p\bar{p}$ collisions at the Fermilab Tevatron Collider. The B_s candidates are reconstructed in the decay chain $B_s \rightarrow J/\psi \phi$, with $J/\psi \rightarrow \mu^+ \mu^-$ and $\phi \rightarrow K^+ K^-$. We determine the mass of the B_s meson to be $M(B_s) = 5.36 \pm 0.03 \text{ GeV}/c^2$. By fitting the proper decay length of the B_s candidates, we obtain the B_s lifetime, $\tau(B_s) = 1.16 \pm 0.42 \text{ ps}$. For simplicity, values are presented with only their statistical uncertainty.

1 Introduction

In 1977, the bottom quark was discovered as a resonance in the dimuon invariant mass spectrum in 400 GeV proton-nucleus collisions at Fermilab [1]. The bottom quark is one of six flavours of quarks described in the Standard Model of Particle Physics (SM); the SM is a theoretical framework that describes particle reactions up to energies achieved by present-day accelerators to a very high precision [2].

The strange B meson (B_s) is a chargeless meson composed of a bottom antiquark (\bar{b}) and a strange quark (s). The production of B_s mesons is driven by the strong force in a two-step process: the production of b-quark pairs from proton-proton collisions and the formation of hadrons through hadronisation [3].

In the SM, the decay rate of quarks via W-emission is parameterised by the Cabibbo-Kobayashi-Maskawa (CKM) quark-mixing matrix. As seen in Figure 1, the $B_s \rightarrow J/\psi \phi$ weak decay mode is via $b \rightarrow \bar{c}s$ transitions. Both this decay and the further decays, $J/\psi \rightarrow \mu^+ \mu^-$ and $\phi \rightarrow K^+ K^-$, can be considered as a two-body decay in which a parent particle decays into two daughter particles.

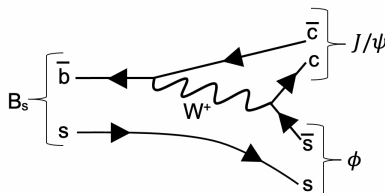


Figure 1: Feynman Diagram for $B_s \rightarrow J/\psi \phi$ Decay

Via relativistic kinematics (working in units where $c \equiv 1$), the invariant mass of the parent particle, M , is given by,

$$M^2 = m_1^2 + m_2^2 + 2(\sqrt{p_1^2 + m_1^2} \sqrt{p_2^2 + m_2^2} - \underline{p}_1 \cdot \underline{p}_2), \quad (1)$$

where m_1 and m_2 are the masses of the two daughter particles and \underline{p}_1 and \underline{p}_2 are their respective momenta.

The decays of neutral B mesons to a charmonium state and a pair of either pions or kaons play an important role in the study of CP violation and mixing [4]. In addition, B hadrons provide valuable information about the CKM matrix, V_{CKM} :

$$\begin{pmatrix} d' \\ s' \\ b' \end{pmatrix} = V_{CKM} \begin{pmatrix} d \\ s \\ b \end{pmatrix} \quad (2)$$

where the CKM matrix,

$$V_{CKM} = \begin{pmatrix} V_{ud} & V_{us} & V_{ub} \\ V_{cd} & V_{cs} & V_{cb} \\ V_{td} & V_{ts} & V_{tb} \end{pmatrix}. \quad (3)$$

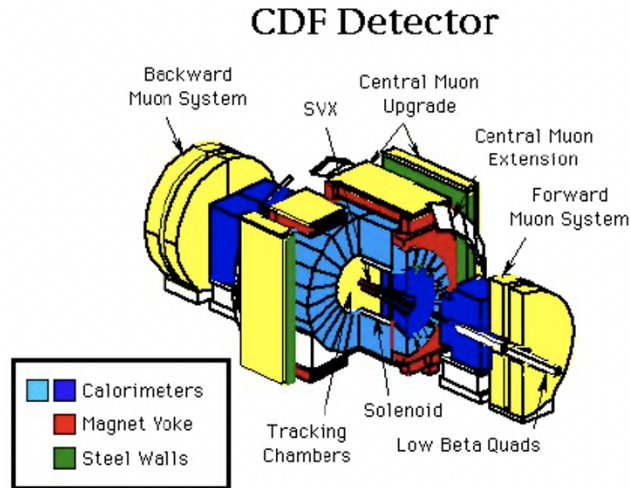


Figure 2: Schematic Diagram of the CDF Detector [5]

B decays determine five of the nine CKM matrix elements: V_{cb} , V_{ub} , V_{td} , V_{ts} , and V_{tb} .

2 Detector

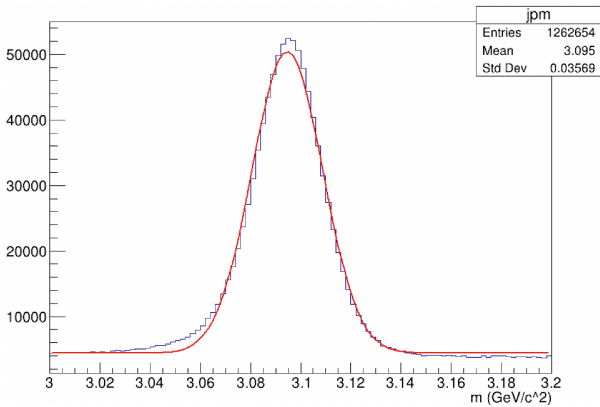
The Collider Detector at Fermilab (CDF) detector, shown in Figure 2, studies high energy particle collisions from the Tevatron collider, the world's former highest-energy particle accelerator. The Tevatron collided protons and antiprotons beams, circulating in opposite directions around the accelerator, at a centre-of-mass energy of 1.8 TeV.

The CDF detector consists of multiple cylindrical layers that surround the beam pipe. The detector components closest to the interaction point are tracking subsystems. These subsystems enable the momenta of particles, as they pass through a 1.4 T solenoidal magnetic field, to be determined. The silicon vertex detector (SVX) provides directional information with good resolution close to the interaction vertex. It consists of four approximately cylindrical layers of silicon strip detectors outside the beam vacuum pipe and concentric with the beam line [6]. Surrounding the SVX, the Central Tracking Chamber (CTC) is a large cylindrical layer drift chamber with excellent spatial and momentum resolution [7]. Outside of the tracking system there are calorimetry and muon systems, which enable the identity of particle to be determined.

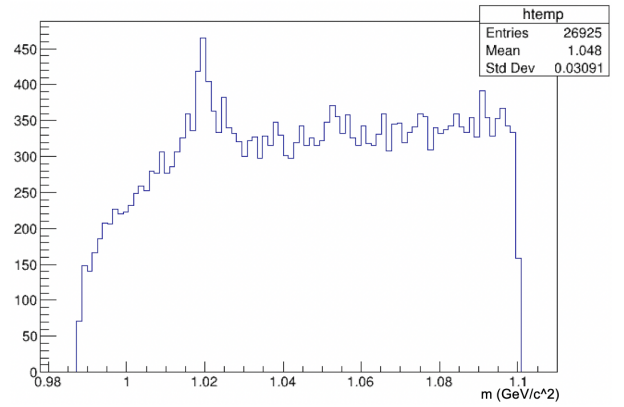
The data in this report, taken from the 1992–1993 run, is based on the inner tracking system measurements only; the identity of particle tracks is not given in the data set. Pairs of oppositely charged muons and kaons produced in collisions are of particular interest in this report. The impact parameter (IP) is defined as the minimum distance of approach of the track with respect to the primary vertex. By selecting tracks with large transverse momentum, p_T , with respect to the proton beam direction, the IP resolution is improved. In this report, systematic uncertainties due to components of the detector are neglected; values are presented with their statistical uncertainty.

3 Event Selection

The reconstruction of $B_s \rightarrow J/\psi \phi$ proceeds by finding $J/\psi \rightarrow \mu^+ \mu^-$ candidates and then combining them with oppositely charged kaons from the $\phi \rightarrow K^+ K^-$ decay. The lifetime of charged kaons is $\tau(K^\pm) \approx 1.2 \times 10^{-8}$ s and for muons is $\tau(\mu^\pm) \approx 2.1 \times 10^{-6}$ s, so making cuts on p_T to be on the order of 1 GeV/c means the probability that the muons or kaons decay within the detector is negligible.



(a) The Invariant Mass Distribution of Oppositely Charged Muon Pairs



(b) The Invariant Mass Distribution of Oppositely Charged Kaon Pairs

Figure 3: Invariant Mass of Secondary Decays

3.1 $J/\psi \rightarrow \mu^+\mu^-$

Using Equation 1, the dimuon mass from possible muon pairs with opposite charges, both with $p_T > 0.5$ GeV/c, have been calculated. Figure 3a shows there is a dominant peak centred around the 3.096 ± 0.011 GeV/c²; this is where we expect to find the J/ψ peak. Cuts are made around this peak so that $M(J/\psi) > 3.07$ GeV/c² and $M(J/\psi) < 3.12$ GeV/c² to remove the some of the background in the tails of the distribution. The $\mu^+\mu^-$ combinations are then constrained to the J/ψ for subsequent use in event reconstruction [8].

3.1.1 $\phi \rightarrow K^+K^-$

Similarly, the dikaon mass from possible kaon pairs with opposite charges gives the distribution found in Figure 3b. In addition to the previous cuts made on the mass of the J/ψ and the muons, the transverse momentum of both of the kaons is made so that $p_T > 1.5$ GeV/c. The decrease in the background for masses below the ϕ peak is limited, by Equation 1, to be twice that of the rest mass of a kaon, $M(K^\pm) = 0.4937$ GeV/c². In Figure 3b, a peak due to the $\phi \rightarrow K^+K^-$ decay mode is centred around 1.019 ± 0.003 GeV/c². Cuts are made around this peak so that $M(\phi) > 1.015$ GeV/c² and $M(\phi) < 1.025$ GeV/c² to remove some of the background. The large amounts of background is due to many of these pairs of oppositely charged particles being muons that are incorrectly reconstructed as kaons, since many more muons are produced than kaons in collisions.

4 Mass of Strange B meson

Cuts on the transverse momenta of J/ψ and ϕ are made so that $p_T > 4$ GeV/c. Also, tighter cuts on the kaons are made so that their $p_T > 2$ GeV/c. The invariant mass distribution of the B_s meson is calculated using Equation 1. Figure 4 shows a prominent peak that is due to the decay of the B_s meson. Fitting a Gaussian to this peak and background, we find the mass of the B_s meson to be $M(B_s) = 5.36 \pm 0.03$ GeV/c².

5 Lifetime of Strange B meson

In this section, cuts on the kaons of $p_T > 1.5$ GeV/c are made. In addition, cuts around the B_s meson of $M(B_s) > 5.3$ GeV/c² and $M(B_s) < 5.4$ GeV/c² are made. We use a vertex fitting algorithm to calculate the proper decay length of the B_s mesons found. Vertex fitting takes a number of tracks which we think came from a single vertex and fit to find the common point of origin, taking into account the pull required to match up the tracks through a linear square fit [9]. Since both the daughter particles of the decay of B_s meson decay into two more particles, we expect the topology of the decay to be two pairs of tracks originating from separate vertices.

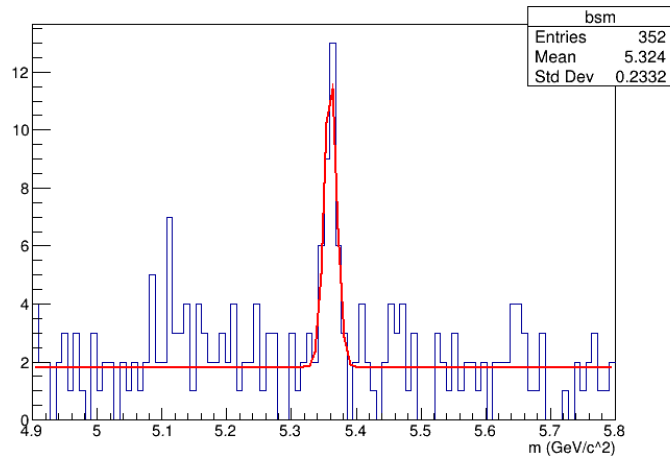


Figure 4: The Invariant Mass Distribution of the B_s Meson

In Figure 5, we fit a Gaussian for the background and an exponential decay for the B_s mesons decaying to the positive proper decay lengths of the B_s mesons. We measure the B_s lifetime to be $\tau(B_s) = 1.16 \pm 0.42$ ps. Some unphysical negative decay lengths are found that are due to background. Ideally a better fit would be an exponential convoluted with a Gaussian over all decay lengths to model background events and an exponential decay over positive decay lengths to model the B_s mesons decay.

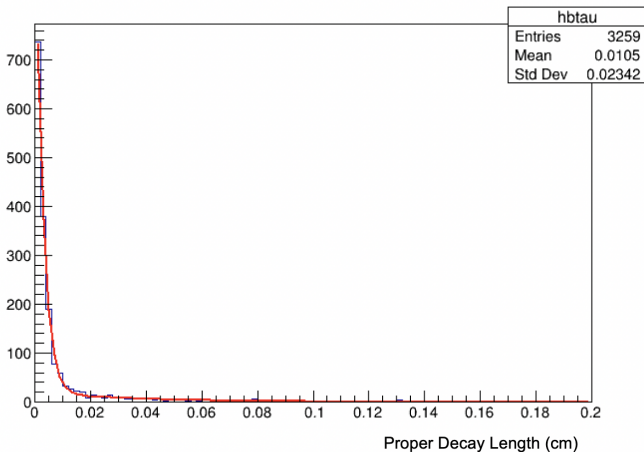


Figure 5: Proper Decay Length of the B_s Meson

6 Conclusions

We observe a prominent peak for the invariant mass of the B_s meson to be $M(B_s) = 5.36 \pm 0.03 \text{ GeV}/c^2$. Reconstructing the same decay chain for proton-proton collisions at 7 TeV, data from the LHCb found the mass of the B_s meson to be $M(B_s) = 5.36690 \pm 0.00028 \text{ (stat)} \pm 0.00031 \text{ (syst)} \text{ GeV}/c^2$ [10], where both the statistical and systematic uncertainties are given separately. These values are in agreement, but the larger LHCb data set results in a much smaller statistical uncertainty. It should be noted that this report neglects the systematic uncertainty of measurements. Future analysis should include a proper treatment of the systematic uncertainties that arise from a variety of sources: trigger uncertainty, reconstruction efficiency, scale efficiency, and track momentum efficiency. However, this data sample is likely to be statistically limited, due to its relatively small size. Increasing the size of the data sample would increase the confidence of the statistical significance of this peak by reducing the statistical uncertainty.

In addition, we obtain the lifetime of the B_s meson to be $\tau(B_s) = 1.16 \pm 0.42$ ps. Using another data sample of 1.8 TeV $p\bar{p}$ collisions collected by the CDF detector, the B_s lifetime was determined to be $\tau(B_s) = 1.42^{+0.27}_{-0.23} \text{ (stat)} \pm 0.00031 \text{ (syst)} \text{ ps}$ [11]. These values are in agreement. To reduce the statistical uncertainty on the lifetime measurement, future analysis should use a larger data sample and implement

an improved method of fitting the background for the proper decay length of the B_s mesons.

References

- [1] Herb S. W. et al. Observation of a Dimuon Resonance at 9.5 GeV in 400-GeV Proton-Nucleus Collisions. *Phys. Rev. Lett.* 39, 252 (1977)
- [2] Ellis J. Outstanding questions: physics beyond the Standard Model. *Philosophical Transactions of the Royal Society A* 370, 1961 (2012)
- [3] Cerizza, G. *Measurement of Production and Decay Properties of Bs Mesons Decaying into J/Psi Phi with the CMS Detector at the LHC*. PhD. University of Tennessee. (2012)
- [4] Adeva B. et al. First Observation of the $B^0 \rightarrow J/\psi K^+K^-$ and search for $B^0 \rightarrow J/\psi \phi$ decays. *Phys. Rev. D.* 88, 072005 (2013)
- [5] CDF. *3-Dimensional COLOR View of CDF in Collider Run I, 1992-96*. [image] (1992). Available at: https://www-cdf.fnal.gov/experiment/drawings/detector_drawings.html [Accessed 14 December 2020]
- [6] Abe F. et al. Observation of Bc mesons in pp collisions at $\sqrt{s}= 1.8$ TeV. *Phys. Rev. D.* 58, 112004 (1998)
- [7] Abe F. et al. The CDF Detector: An Overview. *Nuclear Instruments and Methods in Physics Research Section A: Accelerators, Spectrometers, Detectors and Associated Equipment* 271, 3 (1988)
- [8] Beringer J. et al. Review of Particle Physics. *Phys. Rev. D.* 86, 010001 (2012)
- [9] Huffman T. *NP10*. (2011). Available at: <https://www-teaching.physics.ox.ac.uk> [Accessed 14 December 2020]
- [10] Patrignani, C. Review of Particle Physics. *Chin. Phys. C* 40, 100001 (2016)
- [11] Abe F. et al. Measurement of the Bs meson lifetime. *Phys. Rev. D.* 74, 4988 (1995)